Review

J. Electrochem. Sci. Technol., **2023**, *14(1)*, *1-14*

Recent Applications of Molecularly Imprinted Polymers (MIPs) on Screen-Printed Electrodes for Pesticide Detection

Adilah Mohamed Nageib[1], Amanatuzzakiah Abdul Halim[1*], Anis Nurashikin Nordin[2], and Fathilah Ali[1]

[1]*Department of Chemical Engineering and Sustainability, Faculty of Engineering, International Islamic University Malaysia (IIUM), Kuala Lumpur, Malaysia*

[2]*Department of Electrical and Computer Engineering, Faculty of Engineering, International Islamic University Malaysia (IIUM), Kuala Lumpur, Malaysia*

ABSTRACT

The overuse of pesticides in agricultural sectors exposes people to food contamination. Pesticides are toxic to humans and can have both acute and chronic health effects. To protect food consumers from the adverse effects of pesticides, a rapid monitoring system of the residues is in dire need. Molecularly imprinted polymer (MIP) on a screen-printed electrode (SPE) is a leading and promising electrochemical sensing approach for the detection of several residues including pesticides. Despite the huge development in analytical instrumentation developed for contaminant detection in recent years such as HPLC and GC/MS, these conventional techniques are time-consuming and labor-intensive. Additionally, the imprinted SPE detection system offers a simple portable setup where all electrodes are integrated into a single strip, and a more affordable approach compared to MIP attached to traditional rod electrodes. Recently, numerous reviews have been published on the production and sensing applications of MIPs however, the research field lacks reviews on the use of MIPs on electrochemical sensors utilizing the SPE technology. This paper presents a distinguished overview of the MIP technique used on bare and modified SPEs for the detection of pesticides from four recent publications which are malathion, chlorpyrifos, paraoxon and cyhexatin. Different molecular imprint routes were used to prepare these biomimetic sensors including solution polymerization, thermal polymerization, and electropolymerization. The unique characteristics of each MIP-modified SPE are discussed and the comparison among the findings of the papers is critically reviewed.

Keywords : Pesticides, Molecularly imprinted polymer, Screen-printed electrode, Sensor

Received : 8 August 2022, Accepted : 8 October 2022

1. Introduction

The steady increase in the world's population has led to the rise in the utilization of pesticides in agronomics and farming processes to combat pests, protect crops and fulfill the worldwide food supply. Organophosphates (OPs) pesticides are chemical compounds containing phosphorous atoms double-bonded either with an oxygen atom (via phosphoryl bond) or a sulphur atom (via thiophosphoryl bond). OPs represent one of the most highly-produced and commonly utilized pesticides, which represents globally around 34% and 38% of pesticides sales and consumption, respectively [1–3]. The common OP pesticides used in farming and residential applications are chlorpyrifos and malathion with approximate annual usage of 80 million pounds of OP pesticides in the United States, with 75% of their use in agriculture, which are considered hazardous by the WHO that are classified under Class IV & Ib and Class III respectively [4]. Additionally, there are regulation sets by World Health Organization (WHO) for pesticide usage as illustrated in Table 1 based on common OP compounds and Lethal Dose 50 (LD50) toxicities level.

Despite the high demand in the market, OPs and most pesticides bring harm to living beings and continue to remain in the environment over a long period. The risk of long-term exposure to pesticides could be very poisonous, mutagenic, carcinogenic,

*E-mail address: amana@iium.edu.my

DOI: https://doi.org/10.33961/jecst.2022.00654

Table 1. OP pesticides structures and LD50 toxicities [1,4,5]

No.	OP name	LD_{50} (mg/kg)	WHO acute hazard
1	Parathion	13	Ia
2	Azinphos-methyl	16	Ib
3	Malathion	c2100	III
4	Dichlorvos	57-108	Ib
5	Chlorpyrifos	135	II

and tumorigenic for humans [6]. Moreover, the frequent use of OPs on farms leads to the exposure of the consumers to chemical toxins as the pesticide residues retain on crops and livestock causing ecological defilement by affecting human health through overstimulating the neurotransmission framework as it metabolizes quite rapidly in humans [2,7]. One of the studies reported that children left unprotected from OP residues were more prone to attention deficit hyperactivity disorder (ADHD) diagnosis [8]. A previous study showed that OP pesticides were the cause of more than 15,000 fatalities and specifically 3 million cases of sharp food intoxication yearly via agriculture staff and rural societies around the world [9].

Analytical methods were developed for the determination of pesticide residues in different samples as an alternative to natural recognition systems (enzymes, antibodies, etc.) in various applications [10,11]. In particular, molecularly imprinted polymer (MIP) offers several advantages which include robust, versatile and low-cost synthesis system that can be integrated into many sensing platforms for detection of various target analytes [10,12–14]. MIPs are synthetic recognition elements producing structurally artificial recognition sites “cavities” in polymeric matrices which are complementary to the analyte-for rebinding to target molecules through a process known as molecular imprinting. During polymerization process, the functional monomer with the aid of a cross-linker and the targeted pesticide acting as a template polymer, react to form a polymer matrix. The template polymer will eventually be extracted and the cavities will be imprinted. The newly formed cavities created are complementary to the pesticide molecule in molecular structure and orientation of functional groups. And for that, MIPs can be deemed as a biomimetic recognition elements [15]. Fig. 1 shows the basic polymerization steps and main components presence in the synthesis of MIP.

MIP’s simple and facile synthesis, structurally tailored recognition features, ability to withstand extreme environments, enhanced thermal/chemical stability and long shelf-life make them suitable for different applications [16,17]. These applications of MIPs can be found in many areas, such as chiral separation by chromatography [18], solid-phase extraction [19,20], catalysis [21], or electrochemical sensing [22,23]. The most commonly used methods for MIP synthesis are bulk polymerization, emulsion polymerization, free radical polymerization, precipitation polymerization, photopolymerization, or electropolymerization [24–27]. For the development of biomimetic sensors, the molecular imprinting on SPE’s surface is classified into three main types; bulk imprinting, surface imprinting (soft lithography, template immobilization and grafting, emulsion), and epitope imprinting [28,29].

A vital component in designing MIP is choosing the suitable monomer with functional groups that can interact with the template molecules to form a polymer complex in the pre-polymerization step. Among the potential monomers, methacrylic acid (MAA), 2-hydroxyethyl methacrylate (HEMA), pyrrole, and acrylamide are frequently applied for non-covalent imprinting because of their great capabilities as a hydrogen bond donor and acceptor [29–31]. β-cyclodextrins was reported to be an attractive alternative over the traditional monomer due to the various possible interactions with templates, water compatibility and chirality [29]. The fixation of a functional monomer around the template molecule is achieved with the aid of a cross-linking agent as shown in Fig. 1. Reducing the concentration of the cross-linker agent results in an unstable mechanical property while increasing it may lower the number of recognition sites per MIP unit mass. Some of the commonly used cross-linkers are triallyl isocyanurate (TAIC), bis (1-(tert-butylperoxy)-1-methylethyl)-benzene (BIBP), and ethylene glycol dimethacrylate (EGDMA) [29].

Screen-Printed Electrodes (SPEs) are miniaturized analytical devices used for the detection of desired analytes that comprises a sensing material (recognition element), which can be a natural bio-recognition element such as enzymes and living cells recognizing the pesticide analyte, or a synthetic recognition element such as MIP. SPE acts as a transducer that con-

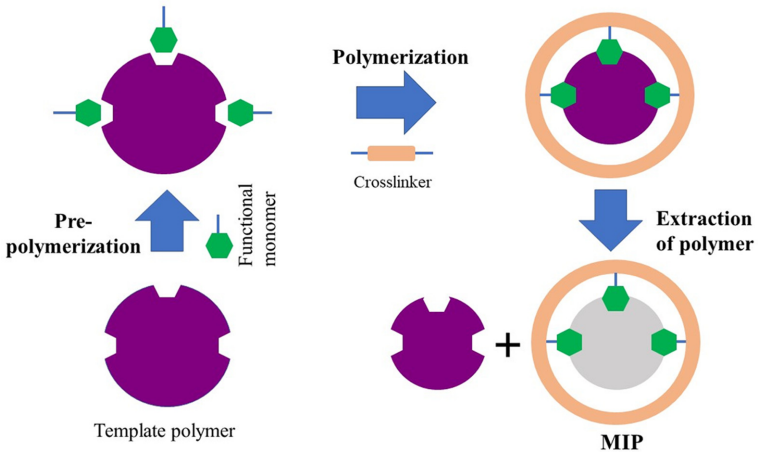

Fig. 1. Two-dimensional schematic diagram for Molecularly Imprinted Polymer (MIP) process

verts a chemical signal of electrochemical reactivity from the interaction of the analyte with the recognition element to an electric current. The main advantages of SPEs over traditional electrodes include simplicity, portability, relatively cheap and mass production capabilities. SPEs have been widely studied on sensing and detection platforms for various applications including pesticides [30,32–34], antibiotics [31,35–37], proteins [38–42], drugs [43–46], and neurotransmitters [47,48].

This review covers the recent applications of molecularly imprinted polymers on screen-printed electrodes for pesticide detection. Four different types of pesticides were selected which are malathion, chlorpyrifos, paraoxon and cyhexatin. From the four recent publications chosen, we discussed in detail the fabrication process of MIP outlining the complexity, successfulness, selectivity, and limit of detection (LOD) of the MIP protocols on different sensing platforms for pesticide detection systems. Furthermore, this review also focuses on exploring diverse aspects of MIPs technique and SPEs platforms including the process, advantages, drawbacks and the significance of the techniques and applications.

2. MIP Fabrication Processes

2.1 Malathion pesticide

Malathion (MAL) is considered to be one of the common broad-spectrum pesticides against a variety of outdoor pests in different agricultural and residential landscapes. Aghoutane *et al.* [32] have developed a screen-printed gold electrode (SPGE) modified with MIP. The commercial three-electrode system SPGE sensor (DropSens. Inc.) was tested with olive oil and fruit samples for the detection of MAL residues. Fig. 2 illustrates the fabrication process of the imprinted SPGE sensor through polymerization and extraction of the template molecule processes. The MIP was synthesized by solution polymerization through incubation of acrylamide as the functional monomer, bisacrylamide as cross-linker and MAL as the template molecule. The reaction was carried out in the presence of TEMED (tetramethylethylenediamine) and ammonium persulfate as catalysts. The synthesized MIP was deposited on the working electrode and detection and quantification of MAL were performed.

To study the electrode's surface morphology, scanning electron microscopy (SEM) with energy dispersive X-Ray spectroscopy (EDS) and atomic force microscopy (AFM) instruments were selected. SEM images and EDS for the bare SPGE electrode revealed a uniform surface indicating the presence of gold (88.86%) (Fig. 3a). The MIP layer on the SPGE surface revealed a thin and rough film with a granular morphology after modifying with the MIP complex showing the uniform deposition of the un-leached polymer on the electrode due to the presence of 35% for carbon (C), 36% for oxygen (O), and 12% of sulfur (S) (Fig. 3b). Meanwhile, a more compact morphology and a relatively smooth surface were shown in the image depicting MIP surface after extraction

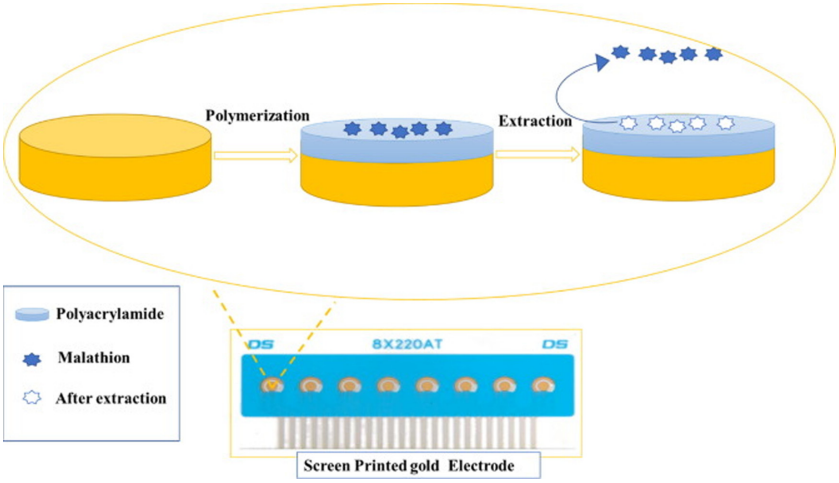

Fig. 2. Fabrication process of SPGE using MIP to detect malathion. Reprinted with permission from [32]. Copyright 2020 Elsevier

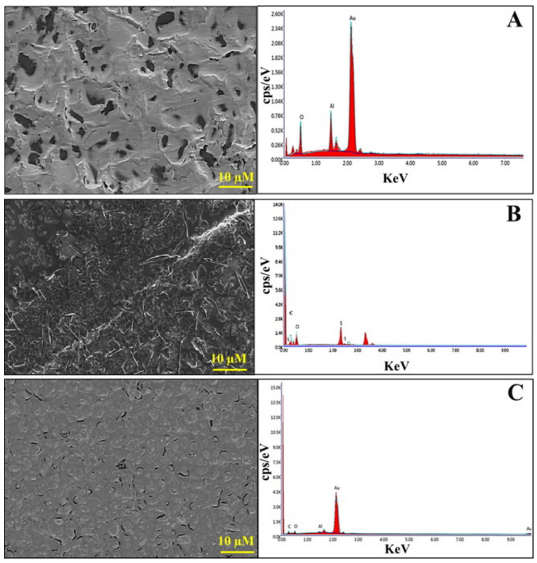

Fig. 3. (a) SEM images and EDS spectra of Bare SPGE; (b) SPGE before MAL extraction; (c) and SPGE after MAL extraction. Reprinted with permission from [32]. Copyright 2020 Elsevier

process (Fig. 3c). This SEM image is in agreement with the EDS data that recorded lower oxygen content (5%) which corresponds to the removal of the MAL molecules from the MIP matrix.

AFM characterization was used to examine the surface roughness of the electrode. After the deposition of the un-leached MIP layer, the surface roughness increased to 764 nm and decreased to 472 nm after the extraction step. The values show the polymer formation in the electrodes and confirm the estimated rise in the roughness of the surface after depositing the polymer layer. The selectivity of the developed MIP sensor towards MAL was examined with another two pesticides (dimethoate (DMT) and fenthion (FEN)) and the control non-imprinted polymer (NIP) using DPV. The observed current responses of the MIP sensor towards MAL were higher than the other interferences where MIP exhibited a value of -0.29 µA, NIP and DMT showed similar current response at -0.026 µA, wherein FEN responded at -0.006 µA.

The summary in Table 2 shows the best limit of detection (LOD) for MAL obtained by the SPGE electrode with MIP at 1.81×10^{-13} M. There were no other reported studies detecting malathion using MIP sensor. However, various sensors with different recognition elements were used, among them are enzyme and aptamer with LOD range between 0.2×10^{-6} M to 0.06×10^{-12} M. Based on the LOD values obtained, the imprinted MIP/SPGE sensor presented the lowest LOD value compared to other sensors developed using different recognition systems indicating high sensitivity that is due to the gold working electrode that has strong adsorption towards the analyte with electrochemical reversibility [49].

2.2 Chlorpyrifos pesticide

Chlorpyrifos is a highly toxic organophosphate (OP) pesticide used for agricultural and non-agricul-

tural purposes (buildings and in other settings) primarily to control foliage and soil-borne insects and arthropod pests [50]. Capoferri et al. [33] have developed an electrochromic SPE sensor using indium tin oxide (ITO) as the working electrode. The sensor was modified with mixture of iridium oxide nanoparticles (IrOx NPs) and molecularly imprinted polypyrrole as a recognition layer and was tested with spiked drinking water samples containing chlorpyrifos. MIP was synthesized and deposited on the SPE in two phases; through electrodeposition of IrOx NPs, followed by thermal polymerization. The electrodeposition of IrOx NPs was carried out by CV at 100 mV/s between -0.7 and +1.0 V for 50 cycles in NaOH solution. Thermal polymerization of polypyrrole (functional monomer) was then performed on the resulting deposited IrOx NPs in the presence of the analyte (chlorpyrifos) creating MIP films onto the surface of the working electrode (ITO). Thermal polymerization was conducted by placing the polymerization solution on the surface of ITO and placed in the oven. The extraction was completed by immersing the MIP electrode in HCl solution.

Detection and quantification were performed through visual and smartphone imaging. The increased amount of chlorpyrifos inside the polymer cavities lowered the conductivity of the functional monomer. Fig. 4a shows the operating principle of the sensor based on the decrease in conductivity of the MIP layer. Direct visual detection was performed with different oxidation potentials. The color changes directly for both positive and negative applied potentials which, correspond to the analyte's concentration based on the number of colored electrodes (Fig. 4b). Through smartphone imaging, the concentration of the analyte was dependent on the color intensity of the electrode at a fixed potential (Fig. 4c).

The selectivity of this sensor for chlorpyrifos was tested with another two different OP analogues (chlorfenvinphos and dichlorvos) between 500 fM to 1 mM through visual detection. At 500 fM, the response of both interferences was 5% compared to chlorpyrifos which was approximately 33%. The responses were higher at 1 mM, which was 42% for both interferences compared with the target analyte reaching nearly 98%. The selectivity results proved that the developed electrochromic sensor exhibits a good selectivity towards chlorpyrifos compared to other OP interferences.

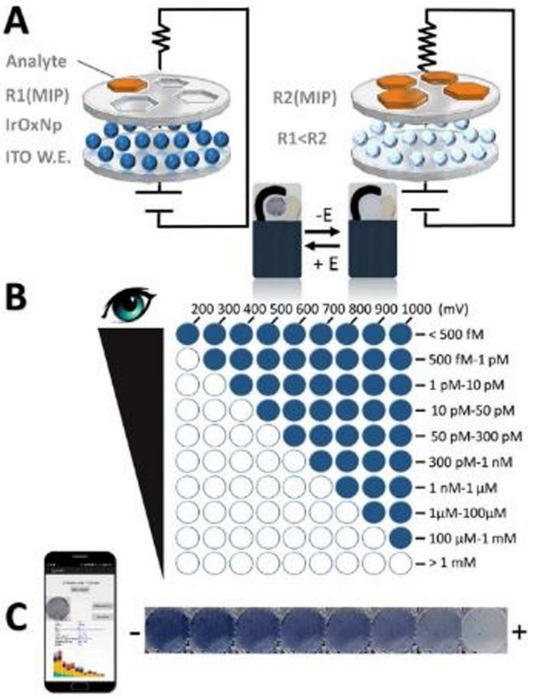

Fig. 4. (a) The working principle of the proposed imprinted IrOx NPs/ITO-SPEs sensor (b) Visual detection of different oxidation potentials and concentration ranges detected and (c) the change of IrOx NPs color intensity with respect to increasing the analyte's amount. Reprinted with permission from [33]. Copyright 2018 American Chemical Society

In Table 2, the LOD for detection of chlorpyrifos using MIP sensors C_3N_4NTs-GQDs/GCE and IrOx NPs/ITO-SPE are comparable which is in the range of $1–2\times10^{-12}$ M. C_3N_4NTs-GQDs/GCE sensor was modified with a carbon nitride nanotubes (C_3N_4NTs), a highly stable allotrope involving weak van der waals interaction between the adjacent C-N layers to form ultra-thin nanosheet [51]. Subsequently, graphene sheets known as graphene quantum dots (GQDs) were added which enhanced the active surface area and improved the overall performance of the sensor. On the other hand, IrOx NPs exhibited electrochemical and electrochromic properties through the reversibly color changes in response to an external applied potential. The detection of chlorpyrtifos was performed based on the correlation between the applied potential to the analyte's concentration range. The color intensity of IrOx NPs turns dark blue upon oxidation and becomes transparent upon reduction related to the increment of chlorpyri-

fos concentration [33]. By choosing ITO as the working electrode material, the electron transfer rate during the redox reaction increases, hence, a lower LOD [52]. The reported value is significantly lower than other reported LOD values using different sensing approaches [53–55].

2.3 Paraoxon pesticide

Paraoxon (PO) is a highly neurotoxic OP pesticide that is widely used to combat pests and is responsible for several poisonings when misused [30]. Li et al. [30] developed a sensor using commercial SPCE (DropSens, Inc.) modified with a conductive nanostructured film consisting of gold nanoparticles (AuNPs). The MIP sensor was then modified with a layer of p-aminothiophenol (PATP) polymer. The performance of the fabricated sensor was tested in spiked apple and cabbage samples with different PO concentrations. The details of the fabrication process are shown in Fig. 5. Fig. 5a, (i) the electrodeposition of AuNPs layer on the surface of the SPCE; (ii) ATP (functional monomer) assembled onto the AuNP layer through self-assembly monolayer (SAM) followed by PO assembly onto it; (iii) the electropolymerization of PATP film on the surface of the electrode in the presence of PO molecules in the polymerization precursor mixture step; (iv)/(v) removal/rebinding of PO molecules on the imprinted sites of the imprinted and modified SPCE sensor. Further self-assembly is demonstrated in Fig. 5b relying on the Au–S bonds and the exposed array of the amino groups towards the solution, forming an ATP SAM.

The electrical current increases with the addition of imprinted PATP film on the surface of the SPCE. There was also an increase in the electrocatalytic reduction current due to the addition of the AuNPs displayed by the one-step electropolymerized imprinted sensor, thus resulting in an increment in the effective surface area and electron transfer. Based on the results, the sensitivity of the imprinted PATP/AuNPs/SPCE can be improved by controlling the imprinted sites at the surface of the AuNPs with a high specific area. For selectivity study, parathion (PT) was used as an interference to verify the affinity of the developed sensor towards PO by testing its DPV responses. The results show high selectivity for PO which is approximately 87% compared to 15% for PT.

Table 2 presents similar LOD values for paraoxon using MIP for both CPE and SPCE decorated with PATP/AuNP using MAA and ATP as monomers, respectively. That proves SPCE strip performance to be as good as CPE with LOD value of 1×10^{-9} M. MIP/SPCE imprinted with PO and cyhexatin pesticides were modified with AuNP [30,34]. To date, AuNPs are known as an ideal choice for an electrochemical sensor's surface modification material and have received massive attention due to their functionalization and unique chemical and physical proper-

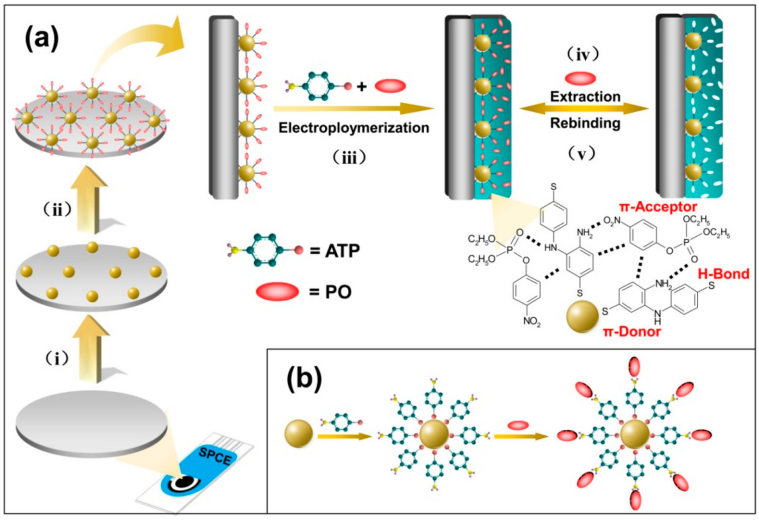

Fig. 5. (a) Preparation of PATP/AuNP/SPCE sensor and the principle for recognition of PO and (b) Adsorption of the ATP molecules on the AuNPs surface. Reprinted with permission from [30]. Copyright 2017 MDPI.

Table 2. Detection of pesticides using various recognition systems

Recognition element	Sensing platform	LOD (M)	Reference
	Malathion		
Enzyme (AChE)	CNT-encapsulated polypyrrole and polyaniline copolymer/GCE	3×10^{-9}	[66]
-	Polyaniline nanofiber and SWCNTs composite/graphite electrode	0.2×10^{-6}	[67]
Aptamer	Cationic polymer and gold nanoparticles aptasensor	0.06×10^{-12}	[68]
MIP	SPGE	1.81×10^{-13}	[32]
	Chlorpyrifos		
Enzyme (AChE)	EμAD of Zinc based Metal Organic Framework/gold μE	1.7×10^{-5}	[53]
-	Nano-TiO_2/ cellulose acetate composite/GCE	4.4×10^{-6}	[54]
Enzyme (AChE)	1-butyl-3- methylimidazolium tetrafluoroborate /MWCNT/composite gel thiocholine	4×10^{-9}	[55]
MIP	C_3N_4NTs-GQDs/GCE	2.0×10^{-12}	[51]
MIP	IrOx NPs-ITO/SPE	1×10^{-12}	[33]
	Paraoxon		
Enzyme (AChE)	HGO/GCE	5.7×10^{-9}	[57]
Enzyme (OPH)	Nanomagnet-silica core-shell/nanobiosensor	5×10^{-6}	[58]
Enzyme (BChE)	Prussian blue nanoparticles/graphite SPE	3.63×10^{-9}	[59]
MIP	CPE	1.0×10^{-9}	[69]
MIP	ATP–AuNPs/SPCE	1.0×10^{-9}	[30]
	Cyhexatin		
MIP (MAA)	AuNPs/ERGO/SPCE	4.41×10^{-10}	[60]
MIP (O-ATP)		5.18×10^{-10}	[34]

*AChE: Acetylcholinesterase; CNT: Carbon nanotube; GCE: Glassy carbon electrode; SWCNT: Single-walled carbon nanotube; EμAD: Electrochemical micro Analytical Device; μE: microelectrode; HGO: Holey graphene oxide; TiO_2: Titanium dioxide; MWCNT: Single-walled carbon nanotube; OPH: organophosphorous hydrolase; BChE: Butylcholinesterase; CPE: Carbon paste electrodes.

ties, such as high surface-to-volume ratio, excellent electron-transfer capability and high electrode conductivity resulting in low limits of detection of the analytes [56]. The presence of AuNP as the backbone layer to the MIP sensor resulted in faster polymerization, due to the higher surface area exposed at the interface with the MIP solution [10]. For paraoxon detection, the resulting imprinted PATP/AuNPs/SPCE possesses high sensitivity, affinity, and selectivity toward the PO [30]. The tested LOD value is relatively in the same range compared to other enzyme-based biosensors [57–59] in Table 2.

2.4 Cyhexatin pesticide

Cyhexatin (CYT) is an organotin compound, which is a common organometallic pesticide that is used widely in agricultural production to combat pests. Zhang et al. [34] developed an MIP sensor (Shanghai Mumei Electronics Technology Co., Ltd.) via self-assembly and electropolymerization of o-aminothiophenol (O-ATP) as a functional monomer for detection of CYT. The first layer of the sensor was modified through electrodeposition of electrochemical reduction graphene oxide (ERGO)-modified on SPCE (AuNPs/ERGO/SPCE). GO suspension on the electrode's surface was dried at 40°C and a potential of -1.3 V was applied for the electrodeposition process. The ERGO/SPCE was further modified via the deposition of gold nanoparticles (AuNPs) using constant potential. Electropolymerization was the method chosen to synthesize the MIP film over the AuNPs/ERGO/SPCE surface. Fig. 6 explains the

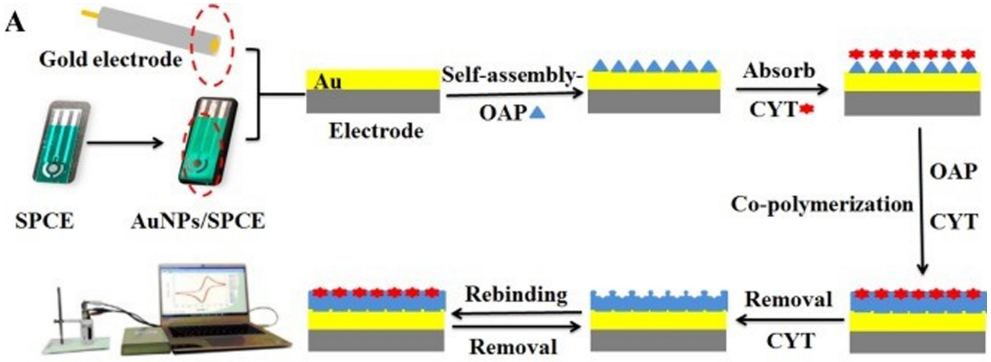

Fig. 6. Schematic diagram for the preparation of MIP sensors to detect CYT. Reprinted with permission from [34]. Copyright 2019 Elsevier

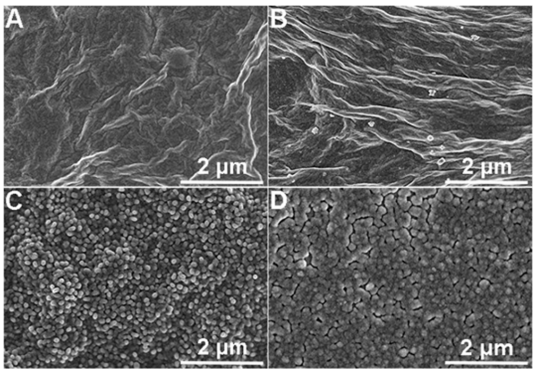

Fig. 7. (a) The SEM photomicrographs of plain SPCE; (b) ERGO/SPCE; (c) AuNP/ERGO/SPCE; and (d) MIP-modified AuNP/ERGO/SPCE. Reprinted with permission from [34]. Copyright 2019 Elsevier

MIP film fabrication by four-step approaches. The AuNPs/ERGO/SPCE was immersed in an O-ATP solution in methanol. After washing the electrode with ethanol and double deionized water (DDW), it was then immersed in a solution of CYT in methanol. The process of electropolymerization of the sensor started with the immersing of the assembled electrodes in the imprinted polymerization solution, and was scanned by CV with a potential range from -0.4 to +0.8 V. Then, the electrode was immersed in dodecanethiol (DDE) methanol solution to seal the blank surface. Finally, the CYT molecules were extracted from the PATP cavities through CV at a potential range between -0.5 to +1.3 V and a scan rate of 100 mV/s to achieve the current response at the potential +1.1 V.

The morphology of the MIP film was characterized by SEM as shown in Fig. 7. The addition of ERGO over SPCE's surface (Fig. 7b) increased the roughness and frills compared to bare SPCE (Fig. 7a). Subsequently, AuNP film was added which can be observed on the surface of the electrode (Fig. 7c). And finally, the completed modified working electrode with the addition of the AuNP/ERGO (Fig. 7d).

Three organotin pesticides were chosen to verify the selectivity of this sensor towards CYT which were azocyclotin, fenbutatin oxide, and fentin hydroxide. The peak current ratio is calculated by Eq. (1).

$$\Delta I/I_0 = (I_0 - I_c)/I_0 \quad (1)$$

The purpose of applying this equation was to verify the specific bindings of the MIP sensor, where I_0 and I_c are the peak current before absorbtion of the analytes and after by the MIP sensor, respectively. The ratio showed the highest trend for CYT at nearly 54% and 16% for azocyclotin, 18% for fentin hydroxide, and 22.5% for fenbutatin oxide. There were linear responses observed between CYT concentration and the response of the MIP sensor from 1 to 500 ng/mL (AuNP/EGRO/SPCE).

Illustrated in Table 2, the LOD values for MIP-cyhexatin on SPCE modified with ERGO/AuNP using 2 different monomers (MAA and ATP) with comparable values which are 4.41×10^{-10} M and 5.18×10^{-10} M respectively [34,60]. The imprinting of MIP cyhexatin is achieved by the interaction of hydrogen bond between the oxygen atom of cyhexatin and the amino groups ($-NH_2$) that are present in both O-ATP and MAA, which could increase the

number of imprinted sites and the sensitivity of the imprinted sensor. Cyhexatin was detected by a sensor modified with a hybrid composite of AuNPs and ERGO. ERGO provides larger specific surface area with electrocatalytic ability and excellent hydrophilicity properties. However, reduced conductivity was observed when the sensor was modified with ERGO material alone [61]. To overcome this issue, a composite hybrid of ERGO sheets stacked with AuNPs were added. Moreover, the wrinkled ERGO sheets provide a 3D network scaffold for the AuNPs to adhere and promote rapid heterogeneous electron transfer [34,61]. The highly electroactive surface area and enhnced heterogeneous electron transfer ability of ERGO flakes contributes to the increase in the anodic peak current response having a π–π interaction, leading to a large scale redox conversion [62]. The CV response of ERGO/SPCE increased sharply compared with the GO/SPCE which indicated the reduction of GO had removed the oxygen group of GO and increased the conductivity of GO. In addition, the CV response of AuNPs/ERGO/SPCE was higher compared to CV of AuNPs/SPCE which demonstrated the significance of both AuNPs and ERGO in improving the overall performance of the sensor [34]. Apart from MIP-SPE based sensor, alternative method such as chromatography was used for cyhexatin detected in fruit and vegetable samples with LOD values of 6.9×10^{-15} M [63] and 3.5×10^{-16} M [64,65]. Table 2 presents the summary of the LOD values for the four pesticides and other studies using a variety of SPE platforms using different biorecognition elements.

3. Overall Comparison and Critical Review

The world's population is rapidly and continuously expanding which led to the excessive use of pesticides in the agricultural sector to meet the global food demand [2]. Pesticide residues are highly neurotoxic to humans. It can be harmful through absorption, inhalation, ingestion, and skin penetration [70]; hence, pesticide residue detection is of great concern. Herein, we reviewed selected reports related to the use of MIPs-based electrochemical sensors for pesticide detection. Table 3 summarizes the analytical parameters and categories of MIP sensors used to distinguish between the reported pesticide detection works. Several categories were considered which are polymerization method, functional monomer, sensing platform, LOD and selectivity.

MIP can be produced via various methods of polymerization such as bulk, free radical, and electropolymerization which can lead to different results in terms of sensitivity, selectivity, and the sensor's performance due to diversified protocols and materials used [27,29]. According to the summary in Table 3, three types of polymerization procedures were used based on a set of reagents for different analytes which are solution, thermal, and electropolymerization.

Malathion was detected by MIP synthesized via solution polymerization reaction. This reaction requires a solvent, a suitable free radical initiator, or a catalyst that is consumed in the reaction while catalysts are regenerated after the completion of the reaction [71,72]. The catalyst used for malathion-MIP was ammonium persulfate, which is an oxidizing agent that is often used with TEMED to catalyze the polymerization of acrylamide and bisacrylamide [32]. To improve heat transfer, the solution polymerization technique uses solvent as a heat sink [71–73] which has to be carefully selected to avoid chain transfer reactions that may limit the growth of the

Table 3. Comparison table for pesticide detection using various MIP sensing methods and platforms

Pesticide	Sensing platform	Polymerization method	Functional monomer	LOD (M)	Selectivity
Malathion [32]	SPGE	Solution polymerization	Acrylamide	1.81×10^{-13}	94%[1]
Chlorpyrifos [33]	IrOx NPs/ITO-SPE	Thermal polymerization	Pyrrole	1×10^{-12}	79%[2]
Paraoxon [30]	PATP/AuNPs/SPCE	Electropolymerization	PATP	1×10^{-9}	85%[3]
Cyhexatin [34]	AuNPs/ERGO/SPCE	Electropolymerization	(O-ATP)	5.18×10^{-10}	67%[4]

[1]Malathion selectivity was calculated at a concentration of 3 pg/ml with respect to fenthion
[2]Chlorpyrifos selectivity was calculated at a concentration of 1 mM with respect to chlorfenvinphos
[3]Paraoxon selectivity was calculated at a concentration of 50 μM with respect to parathion
[4]Cyhexatin selectivity was calculated at a concentration of 0.20 ng/ml with respect to azacyclotin

polymer [74]. In addition, neutral or ionic monomers are mixed with crosslinking agents and the polymerization can be initiated thermally by plasma, ultrasound, redox initiation, ultraviolet or ionizing-irradiation [73,75]. Improved binding affinity of MAL-MIP was observed at temperature of 74°C due to the increase in the interaction strength between complementary acrylamide functional groups (*i.e.* amide) with the malathion (*i.e.* carboxyethyl ester) and the polymer embedded within the imprinted cavity [32].

Chlorpyrifos detection using MIP-based sensor was developed by thermal polymerization at 90°C for 1 min. A thermal polymerization is a reaction in which the monomer is converted to the polymer by thermal energy. Synthesis of several polymers including methyl methacrylate (MMA), n-Butyl Acrylate (n-BA) and Ethyl Acrylate (EA) were conducted at various temperature ranging from 40–200°C with polymerization time from 1 minute to 24 hours [33,76–80]. The degree of polymerization increases with temperature, reaction time and monomer concentration [75].

Electropolymerization was the synthesis method used to detect both paraoxon and cyhexatin. Electropolymerization is a deposition procedure in which a conductive polymer layer is formed or coated upon an electrode/supporting substrate material in the presence of the target template. The majority of electrochemical MIP sensors were developed via free radical polymerization while another 18% of them were produced by electropolymerization [27]. This method offers several advantages over the traditional method e.g. free-radical polymerization, such as short preparation time, excellent adherence to the transducer surface, good control over the layer thickness, morphology and the possibility of aqueous preparation. The detection limits of the sensors prepared using this method reported good sensitivity and selectivity for the target analytes in the range values of nano-molars [27,81,82].

Li *et al.* (2017) performed electropolymerization on paraoxon by seven cyclic scanning from -0.2 to +0.6 V at a at a scan rate (ν) of 0.05 V/s [30]. Whereas, Zhang *et al.* (2018) conducted electropolymerization at a potential range from -0.4 to +0.8 V at a scan rate of 0.1 V/s [34]. The typical potential range usually ranges between -0.2 to +1 V to eliminate the influence of other side reactions [83,84]. The cyclic voltammetry experiment is typically conducted at a specified scan rate. However, varying scan rate itself can provide insights into the reaction mechanism by which polymerisation takes place on the electrode surface. Any specified scan rate determines how fast the applied potential is varied with time during each cycle. Increasing scan rate therefore indicates changing the voltage faster over time, which could implicate the kinetics of charge transfer onto the monomers during the polymerisation process. Changing scan rate, in turn, could affect the magnitude and phase of the peak current produced in the cyclic voltammetry experiment. The effect of changing scan rate on the peak current amplitude can be modelled and plotted through the Randles-Sevcik Equation [49]. A linear correlation between peak current and the square-root scan rate could suggest that the layer formation on the electrode surface is diffusion-controlled. A study showed a linear dependency of the anodic peak current densities which corresponds to the formation of the polymer films Poly-orthochlorophenol (POCP) and Poly-orthohydroxy phenol (POHP) repetitively versus the $\nu^{0.5}$. The correlation coefficient (R^2) was shown to be greater than 0.9 but not equal to 1.0, suggesting that the diffusion of the reacting species to the polymer film/solution interface in a partially diffusion-control process [85]. In addition, the thickness of polymer films can be controlled by varying the number of repetitive cycles [85].

Apart from the advantages offered by the electropolymerization method, some drawbacks were reported. The limitations are on the extraction of the imprinted template and the issue of the optimization conditions for both imprinting and rebinding, such as the solubility and minimization of interactions between the solvent, analyte, and monomer. This method can be improved by the addition of a self-assembled monolayer (SAM). SAM refers to a single layer of molecules adsorbed through chemisorption and exhibits high orientation, molecular ordering and packing density on the sensor's substrate [86]. SAM layer was utilized to detect both paraoxon and cyhexatin and was capable of acting as a "wetting agent" for the polymer produced in the subsequent electropolymerization steps to localize and further improve the imprinted sites on the surface of the MIP layer [10].

The selection of a functional monomer is crucial to provide complementary interactions with the template polymer. Acrylamide (AM) and vinyl esters are

among the most frequently used functional monomers which are suitable for radical polymerization [87]. The monomers are usually divided into acidic, basic, and neutral. The use of various neutral monomers such as acrylic monomers in polymerization resulted in ineffective imprinting [88]. However, improved results have been obtained for acrylamide or its N-alkyl derivatives, especially those using less polar solvents during polymerization [88] resulting in effective imprinting of malathion. One of the best conducting polymers considered for MIP sensors preparation is polypyrrole (PPy) due to its stability, conductive, highly biocompatible, and ability to immobilize with various compounds [33]. Additionally, PPy is water-soluble, which is an important characteristic for the detection of chlorpyrifos as it is mostly found in water samples [27]. The imprinting of the template molecule chlorpyrifos on the PPy film can be explained by non-covalent interactions of a hydrogen bond between the –N group in the pyridine structure of chlorpyrifos and the N–H group of pyrrole. Chlorpyrifos was removed from the PPy film when the imprinted polymer was immersed into the HCl solution. This may be due to the –N group of the pyridine structure having been protonated [89]. This reaction induced mass transfer resistance and accelerated the electron transfer between electrolyte and electrode surface, giving it the advantage of high selectivity over the other metabolites. Besides that, aminothiophenol (ATP) is also considered as one of the suitable monomers for electropolymerization with various benefits including good conductivity, nanostructured, imprinted layer for a constructed sensor through self-assembly [30,34]. The self-assembly of ATP could promote the "wetting agent" on the electrode's surface, hence improving the selective occurrence of electrochemical polymerization.

In the last stage of MIP synthesis, the template polymer is extracted from the polymer matrix leaving what is known as cavities, which are complementary to the template polymer. This is a characteristic that can only be found in MIP, which undoubtedly improves selectivity. To examine the selectivity of the MIP sensor towards the target analyte, the MIP sensor is tested with interferences with very similar molecular structures. For better accuracy, the selectivity test can be done with two and more interferences. MIP sensors have exhibited high selectivity towards respective analytes chlorpyrifos, paraoxon, and cyhexatin. Each MIP sensor exhibited a response higher than 67% in favor of the analyte against their interferences.

4. Conclusions

In this review, the detection of four types of pesticides (malathion, chlorpyrifos, paraoxon, and cyhexatin) using MIP on SPE developed through three different routes of polymerization (solution, thermal, and electropolymerization) have been thoroughly discussed. This review highlighted the synthesis, modification, and application of the developed MIPs for the detection of pesticides in food samples. Various characterization methods were used to analyze the synthesized MIP such as SEM, AFM, CV and DPV. The performance of a MIP/SPE based sensor is dependent on several factors which include polymerization type, functional monomer, and the modification layer. In addition, recent works have shown improved sensor performance through surface modification on the electron transfer and the sensitivity of the MIP sensor.

Although remarkable achievements have been obtained from MIPs in the field of electrochemistry, there are still challenges and opportunities that can be addressed. **(1)** The utilization of MIP sensors can be expanded not only for the detection of molecular analytes but also for biomacromolecules, including viruses. This requires further studies on the nature of the target analytes with fragile and complex structures, solubility, and selectivity [90]. For instance, a rapid detection system would help to contain the spread of COVID-19, a virus infection that can lead to pneumonia caused by severe acute respiratory syndrome [91]. MIP/SPE has the potential to be one of the detection methods apart from the conventional laboratory analysis such as polymerase chain reaction (PCR). COVID-19 Antigen test kit are in high demand due to affordability, easily accessible, easy to use and point of care testing kit. It was indicated that the detection of SARS-CoV-2 (corona virus) can also be performed by selecting appropriate polymer from a library and using corona virus specific aptamer as the recognition element [92]. A comprehensive study of the virus's structure, bindings and interactions are important characteristics of the MIP sensor's detection accuracy. **(2)** Reusability is another issue that can be addressed. MIP/SPEs are generally used as dis-

posable sensors. However, to optimize the usage of MIP/SPE sensors, regeneration can be employed. This sensor can be regenerated through the addition of template extraction solvents. This process is expected to maintain the integration attachment of MIP to the SPE surface without losing its chemical and mechanical stability in extreme environment [90]. **(3)** MIP utilizes corrosive chemicals and hazardous chemicals which are not environmentally friendly and may severely impact the ecosystem. MIP could be prepared using greener reagents to alleviate the intensity of the chemical hazard [90]. The green reagents are chosen for the MIP elements such as for the template (*i.e.* propionamide [93] and daidzein [94]), functional monomer (*i.e.* deep eutectic solvents [95]), cross-linker (*i.e.* 1,4-butanediyl-3,30 - bis-l-vinylimidazolium [96]) and porogenic solvent (*i.e.* ionic liquids [97]). In addition to that, it has been reported in a study that certain types of monomers such as ferrocenylmethyl methacrylate can serve as a functional monomer as well as redox probe which helps in eliminating the use of additional chemicals [98]. On the other hand, stability issue of certain analyte during MIP synthesis can be addressed through the utilization of structural analogue instead of using template analyte [93]. Subsequently, Haupt and Mosbach proposed the concept of a dummy template molecule imprinted polymer based on a green synthesis strategy to reduce the consumption of hazardous/organic reagents [99]. **(4)** There is a lack of evidence of commercial success for MIP-based assays and sensors. The main challenge remains to produce MIPs in large batches that are homogenous in size and shape but also in their affinity towards their target [100]. Thus, the reproducibility of MIP assays and sensors can be explored in terms of homogeneity and affinity to facilitate vast commercial and industrial applications. **(5)** Further improvement of the MIP is necessary not only in terms of the sensor efficiency but also include the cost and expenses incurred during the process, particularly through identifying the optimum polymerization technique or the monomer. The trial-and-error approach in the choice of suitable monomers and experimental conditions for selected templates should be replaced with a more rational approach such as computational and/or combinatorial tools. Some of the software available are Density Functional theory (DFT), GAMESS, Gaussian, LEAPFROG, etc. [87,97].

Acknowlegement

This research was supported by FRGS-RACER Grant Scheme (RACER/1/2019/TK04/UIAM//2) from the Ministry of Higher Education, Malaysia.

References

[1] B. K. Singh and A. Walker, *FEMS Microbiol. Rev.*, **2006**, *30(3)*, 428-471.
[2] K. M. Soropogui, A. T. Jameel, and W. W. A. W. Salim, Indones. *J. Electr. Eng. Informatics*, **2018**, *6(2)*, 161-171.
[3] J. Bao, C. Hou, M. Chen, J. Li, D. Huo, M. Yang, X. Luo, and Y. Lei, *J. Agric. Food Chem.*, **2015**, *63(47)*, 10319-10326.
[4] N. A. Kamaruzaman, Y. H. Leong, M. H. Jaafar, H. R. M. Khan, N. A. A. Rani, M. F. Razali, and M. I. A. Majid, *BMJ Open*, **2020**, *10*, e036048.
[5] T. A. Samuels and S. O. Obare, Advances in Analytical Methods for Organophosphorus Pesticide Detection, in M. Stoytcheva (ed.), *Pesticides in the Modern World - Trends in Pesticides Analysis*, InTechOpen, London, **2011**.
[6] M. F. F. Bernardes, M. Pazin, L. C. Pereira, and D. J. Dorta, Impact of Pesticides on Environmental and Human Health, in A. C. Andreazza, G. Scola (eds.), *Toxicology Studies - Cells, Drugs and Environment*, InTechOpen, London, **2015**.
[7] W. Naksen, T. Prapamontol, A. Mangklabruks, S. Chantara, P. Thavornyutikarn, M. G. Robson, P. B. Ryan, D. B. Barr, and P. Panuwet, *J. Chromatogr. B*, **2016**, *1025*, 92-104.
[8] M. F. Bouchard, D. C. Bellinger, R. O. Wright, and M. G. Weisskopf, *Pediatrics*, **2010**, *125(6)*, e1270-e1277.
[9] B. Dinham, *The Pesticide Hazard: A Global Health and Environmental Audit*, Zed Books, London, **1993**.
[10] C. Malitesta, E. Mazzotta, R. A. Picca, A. Poma, I. Chianella, and S. A. Piletsky, *Anal. Bioanal. Chem.*, **2012**, *402(5)*, 1827-1846.
[11] S. A. Piletsky, S. Alcock, and A. P. F. Turner, *Trends Biotechnol.*, **2001**, *19(1)*, 9-12.
[12] L. Ye and K. Haupt, *Anal. Bioanal. Chem.*, **2004**, *378(8)*,1887-1897.
[13] B. T. S. Bui and K. Haupt, *Anal. Bioanal. Chem.*, **2010**, *398(6)*, 2481-2492.
[14] L. Ye and K. Mosbach, *Chem. Mater.*, **2008**, *20(3)*, 859-868.
[15] J. C. C. Yu and E. P. C. Lai, *Toxins*, **2010**, *2(6)*, 1536-1553.
[16] S. Roshan, A. Mujahid, A. Afzal, I. Nisar, M. N. Ahmad, T. Hussain, and S. Z. Bajwa, *Adv. Polymer Technol.*, **2019**, 9432412.
[17] M. A. Morales and J. M. Halpern, *Bioconjugate Chem.*, **2019**, *29(10)*, 3231-3239.
[18] S. Yang, Y. Wang, Y. Jiang, S. Li, and W. Liu, *Polymers*,

2016, *8(6)*, 216.
[19] Y. A. Olcer, M. Demirkurt, M. M. Demir, and A. E. Eroglu, *RSC Adv.*, **2017**, *7*, 31441-31447.
[20] L.-X. Yi, R. Fang, and G.-H. Chen, *J. Chromatogr. Sci.*, **2013**, *51(7)*, 608-618.
[21] P. S. Sharma, A. Wojnarowicz, W. Kutner, and F. D'Souza, *Molecularly Imprinted Catalysts*, **2016**, 183-210.
[22] B. Feier, A. Blidar, A. Pusta, P. Carciuc, and C. Cristea, *Biosensors*, **2019**, *9(1)*, 31.
[23] A. Sarafraz-Yazdi and N. Razavi, *TrAC - Trends Anal. Chem.*, **2015**, *73*, 81-90.
[24] O. Parkash, C. Y. Yean, and R. H. Shueb, *Diagnostics*, **2014**, *4(4)*, 165-180.
[25] F.-D. Munteanu, A. M. Titoiu, J. L. Marty, and A. Vasilescu, *Sensors*, **2018**, *18(3)*, 901.
[26] M. Peeters, *Austin J. Bios. Bioelectron.*, **2015**, *1(3)*, 1011.
[27] R. D. Crapnell, A. Hudson, C. W. Foster, K. Eersels, B. van Grinsven, T. J. Cleij, C. E. Banks, and M. Peeters, *Sensors*, **2019**, *19(5)*, 1204.
[28] G. Erturk and B. Mattiasson, *Sensors*, **2017**, *17(2)*, 288.
[29] M. I. Malik, H. Shaikh, G. Mustafa, and M. I. Bhanger, *Sep. Purif. Rev.*, **2019**, *48(3)*, 179-219.
[30] S. Li, Q. Luo, Y. Liu, Z. Zhang, G. Shen, H. Wu, A. Chem, X. Liu, and A. Zhang, *Polymers*, **2017**, *9(8)*, 359.
[31] O. Jamieson, T. C. C. Soares, B. A. de Faria, A. Hudson, F. Mecozzi, S. J. Rowley-Neale, C. E. Banks, J. Gruber, K. Novakovic, M. Peeters, and R. D. Crapnell, *Chemosensors*, **2020**, *8(1)*, 5.
[32] Y. Aghoutane, A. Diouf, L. Osterlund, B. Bouchikhi, and N. E. Bari, *Bioelectrochemistry*, **2019**, *132*, 107404.
[33] D. Capoferri, R. Alvarez-diduk, M. del Carlo, D. Compagnone, and A. Merkoci, *Anal. Chem.*, **2018**, *90(9)*, 5850-5856.
[34] C. Zhang, F. Zhao, Y. She, S. Hong, X. Cao, L. Zheng, S. Wang, T. Li, M. Wang, M. Jin, F. Jin, H. Shao, and J. Wang, *Sens. Actuators B Chem.*, **2018**, *284*, 13-22.
[35] A. Zamora-Galvez, A. Ait-Lahcen, L. A. Mercante, E. Morales-Narvaez, A. Amine, and A. Merkoci, *Anal. Chem.*, **2016**, *88(7)*, 3578-3584.
[36] L. Devkota, L. T. Nguyen, T. Thi, and B. Piro, *Electrochim. Acta*, **2018**, *270*, 535-542.
[37] A. G. Ayankojo, J. Reut, V. Ciocan, A. Opik, and V. Syritski, *Talanta*, **2019**, *209*, 120502.
[38] S. C. R. Rebelo, R. Costa, A. T. S. C. Brand, A. F. Silva, M. G. F. Sales, and C. M. Pereira, *Anal. Chim. Acta*, **2019**, *1082*, 126-135.
[39] D. Kumar and B. B. Prasad, *Sens. Actuators B Chem.*, **2012**, *171-172*, 1141-1150.
[40] K. Phonklam, R. Wannapob, W. Sriwimol, P. Thavarungkul, and T. Phairatana, *Sens. Actuators B Chem.*, **2019**, *308*, 127630.
[41] B. V. M. Silva, B. A. G. Rodriguez, G. F. Sales, M. D. P. T. Sotomayor, and R. F. Dutra, *Biosens. Bioelectron.*, **2016**, *77*, 978-985.
[42] A. R. Cardoso, M. H. de Sa, and M. G. F. Sales, *Bioelectrochemistry*, **2019**, *130*, 107287.
[43] A. Motaharian, M. R. M. Hosseini, and K. Naseri, *Sens. Actuators B Chem.*, **2019**, *288*, 356-362.
[44] K. Fu, R. Zhang, J. He, H. Bai, and G. Zhang, *Biosens. Bioelectron.*, **2019**, *143*, 111636.
[45] F. Lopes, J. G. Pacheco, P. Rebelo, and C. Deleruematos, *Sens. Actuators B Chem.*, **2017**, *243*, 745-752.
[46] M. Roushani, Z. Jalilian, and A. Nezhadali, *Colloids Surf. B Biointerfaces*, **2018**, *172*, 594-600.
[47] V. M. Serrano, A. R. Cardoso, M. Diniz, and M. G. F. Sales, *Sens. Actuators B Chem.*, **2020**, *311*, 127902.
[48] M. Amatatongchai, J. Sitanurak, W. Sroysee, S. Sodanat, S. Chairam, P. Jarujamrus, D. Nacapricha, and P. A. Lieberzeit, *Anal. Chim. Acta*, **2019**, *1077*, 255-265.
[49] N. Elgrishi, K. J. Rountree, B. D. McCarthy, E. S. Rountree, T. T. Eisenhart, and J. L. Dempsey, *J. Chem. Educ.*, **2018**, *95(2)*, 197-206.
[50] M. G. Barron and K. B. Woodburn, Ecotoxicology of chlorpyrifos, in G. W. Ware (ed.), *Reviews of Environmental Contamination and Toxicology*, Springer, New York, NY, **1995**, *144.*
[51] M. L. Yola and N. Atar, *J. Electrochem. Soc.*, **2017**, *164(6)*, B223-B229.
[52] J. Shi and D. Marshall, Surface Modification Approaches for Electrochemical Biosensors, in P. A. Serra (ed.), *Biosensors - Emerging Materials and Applications*, InTech, London, **2011**.
[53] S. Nagabooshanam, S. Roy, A. Mathur, I. Mukherjee, S. Krishnamurthy, and L. M. Bharadwaj, *Sci. Rep.*, **2019**, *9*, 19862.
[54] A. Kumaravel and M. Chandrasekaran, *J. Agric. Food Chem.*, **2015**, *63(27)*, 6150-6156.
[55] L. G. Zamfir, L. Rotariu, and C. Bala, *Biosens. Bioelectron.*, **2011**, *26(8)*, 3692-3695.
[56] Sivanesan A. and Abraham J. S., *Ind. Biotechnol.*, **2009**, *9(1)*, 31-36.
[57] Y. P. Li, R. X. Zhao, G. Y. Han, and Y. M. Xiao, *Electroanalysis*, **2018**, *30(10)*, 2258-2264.
[58] R. Khaksarinejad, A. Mohsenifar, T. Rahmani-Cherati, R. Karami, and M. Tabatabaei, *Appl. Biochem. Biotechnol.*, **2015**, *176*, 359-371.
[59] F. Arduini, D. Neagu, V. Scognamiglio, S. Patarino, D. Moscone, and G. Palleschi, *Chemosensors*, **2015**, *3(2)*, 129-145.
[60] C. Zhang, F. Zhao, Y. He, Y. She, S. Hong, J. Ma, M. Wang, Z. Cao, T. Li, A. M. A. Ei-Aty, J. Ping, Y. Ying, and J. Wang, *Microchim. Acta*, **2019**, *186(8)*, 504.
[61] J.-M. Jian, L. Fu, J. Ji, L. Lin, X. Guo, and T.-L. Ren, Sens. *Actuators B Chem.*, **2018**, *262*, 125-136.
[62] S. K. Bhardwaj, R. Chauhan, P. Yadav, S. Ghosh, A. K. Mahapatro, J. Singh, and T. Basu, *Biomater Sci.*, **2019**, *7*, 1598-1606.
[63] Z. Cui, Y. Sun, N. Ge, J. Zhang, Y. Liu, A. Li, and Y. Cao, *Se Pu*, **2014**, *32(8)*, 855-860.
[64] Y. N. Ma, W. J. Gui, and G. N. Zhu, *Anal. Methods*,

2015, *7*, 2108-2113.
[65] Y. Y. Zou and A. Schreiber, *Quantitation and Identification of Organotin Compounds in Food, Water, and Textiles Using LC-MS/MS*, AB Sciex, Concord, Canada, **2012**, 6690212-01.
[66] D. Du, X. Ye, J. Cai, J. Liu, and A. Zhang, *Biosens. Bioelectron.*, **2010**, *25(11)*, 2503-2508.
[67] S. Ebrahim, R. El-Raey, A. Hefnawy, H. Ibrahim, M. Soliman, and T. M. Abdel-Fattah, *Synth. Met.*, **2014**, *190*, 13-19.
[68] R. Bala, M. Kumar, K. Bansal, R. K. Sharma, and N. Wangoo, *Biosens. Bioelectron.*, **2016**, *85*, 445-449.
[69] T. Alizadeh, *Thin Solid Films*, **2010**, *518(21)*, 6099-6106.
[70] J.-L. Wang, Q. Xia, A.-P. Zhang, X.-Y. Hu, and C.-M. Lin, *J. Zhejiang Univ. Sci. B*, **2012**, *13*, 267-273.
[71] G. Odian, *Principles of Polymerization, 4th ed.*, Wiley, **2004**. DOI:10.1002/047147875X
[72] W. I. B. W. Ibrahim and I. M. Mujtaba, *Comput. Aided Chem. Eng.*, **2012**, *31*, 1326-1330.
[73] D. F. Argenta, T. C. dos Santos, A. M. Campos, and T. Caon, Hydrogel Nanocomposite Systems, *Nanocarriers for Drug Delivery,* Elsevier, **2019**, 81-131.
[74] W.-F. Su, Radical Chain Polymerization, *Principles of Polymer Design and Synthesis. Lecture Notes in Chemistry*, Springer, Berlin, Heidelberg, **2013**.
[75] H. Riazi, A. A. Shamsabadi, P. Corcoran, M. C. Grady, A. M. Rappe, and M. Soroush, *Processes*, **2018**, *6(1)*, 3.
[76] H. C. Yu, X. Y. Huang, F. H. Lei, X. C. Tan, Y. C. Wei, and H. Li, *Electrochim. Acta*, **2014**, *141*, 45-50.
[77] N. Yucel, H. Gulen, and P. C. Hatir, *2019 Scientific Meeting on Electrical-Electronics & Biomedical Engineering and Computer Science (EBBT)*, **2019**, 1-4.
[78] T. Pasang and C. Ranganathaiah, *J. Phys.: Conf. Ser.*, **2015**, *618*, 012033.
[79] H.-H. Pan, W.-C. Lee, C.-Y. Hung, and C.-C. Hwang, *J. Chem.*, **2007**, *4*, 632904.
[80] S. I. Khan, R. R. Chillawar, K. K. Tadi, and R.V. Motghare, *Curr. Anal. Chem.*, **2018**, *14(5)*, 474-482.
[81] M. C. Blanco-Lopez, M. J. Lobo-Castanon, A. J. Miranda-Ordieres, and P. Tunon-Blanco, *TrAC – Trends Anal. Chem.*, **2004**, *23(1)*, 36-48.
[82] M. A. Beluomini, J. L. da Silva, A. C. de Sa, E. Buffon, T. C. Pereira, and N. R. Stradiotto, *J Electroanal. Chem.*, **2019**, *840*, 343-366.
[83] E. Pratiwi, A. Mulyasuryani, and A. Sabarudin, *J. Pure Appl. Chem. Res.*, **2018**, *7(1)*, 12-18.
[84] M. Babaiee, M. Pakshir, and B. Hashemi, *Synth. Met.*, **2015**, *199*, 110-120.
[85] S. M. Sayyah, A. B. Khaliel, R. E. Azooz, and F. Mohame, Electropolymerization of Some Ortho-Substituted Phenol Derivatives on Pt-Electrode from Aqueous Acidic Solution; Kinetics, Mechanism, Electrochemical Studies and Characterization of the Polymer Obtained, *Electropolymerization*, IntechOpen, **2011**.
[86] V. Ganesh, S. K. Pal, S. Kumar, and V. Lakshminarayanan, *Electrochim. Acta*, **2006**, *52(9)*, 194-321.
[87] E. Mavroudakis, D. Cuccato, and D. Moscatelli, Determination of Reaction Rate Coefficients in Free-Radical Polymerization Using Density Functional Theory, *Computational Quantum Chemistry,* Elsevier, **2019**, 47-98.
[88] M. Guć and G. Schroeder, *World J. Res. Rev.*, **2017**, *5(6)*, 36-47.
[89] Z. O. Uygun and Y. Dilgin, *Sens. Actuators B Chem.*, **2013**, *188*, 78-84.
[90] B. Cui, P. Liu, X. Liu, S. Liu, and Z. Zhang, *J. Mater. Res. Technol.*, **2020**, *9(6)*, 12568-12584.
[91] B. Huang, R. Ling, Y. Cheng, J. Wen, Y. Dai, W. Huang, S. Zhang, X. Lu, Y. Luo, and Y. Jiang, *Mol. Ther. - Methods Clin. Dev.*, **2020**, *18*, 367-375.
[92] T. N. Chatterjee and R. Bandyopadhyay, Trans. *Indian Natl. Acad. Eng.*, **2020**, *5(2)*, 225-228.
[93] F. Ning, T. Qiu, Q. Wang, H. Peng, Y. Li, X. Wu, Z. Zhang, L. Chem, and H. Xiong, *Food Chem.*, **2017**, *221*, 1797-1804.
[94] X. Sun, J. Wang, Y. Li, J. Yang, J. Jin, S. M. Shah, and J. Chen, *J. Chromatogr. A*, **2014**, *1359*, 1-7.
[95] X. Li and K. H. Row, *J. Chromatogr. B*, **2017**, *1068-1069*, 56-63.
[96] X. Zhu, Y. Zeng, Z. Zhang, Y. Yang, Y. Zhai, H. Wang, L. Liu, J. Hu, and L. Li, *Biosens. Bioelectron.*, **2018**, *108*, 38-45.
[97] L. M. Madikizela, S. Ncube, and L. Chimuka, *Compr. Anal. Chem.*, **2019**, *86*, 337-364.
[98] V. M. Ekomo, C. Branger, R. Bikanga, A. Florea, G. Istamboulie, C. Calas-Blanchard, T. Noguer, A. Sarbu, and H. Brisset, *Biosens. Bioelectron.*, **2018**, *112*, 156-161.
[99] M. Gao, Y. Gao, G. Chen, X. Huang, X. Xu, J. Lv, J. Wang, D. Xu, and G. Liu, *Front Chem.*, **2020**, *8*, 1-20.
[100] J. W. Lowdon, H. Dilien, P. Singla, M. Peeters, T. J. Cleiji, B. van Grinsven, and K. Eersels, *Sens. Actuators B Chem.*, **2020**, *325*, 128973.